Solar-Terrestrial Physics. 2025, vol. 11, iss. 4, pp. 97–103. DOI: 10.12737/stp-114202510. © 2025 A.R. Polyakov, B. Tsegmed. Published by INFRA-M Academic Publishing House

DOI: 10.12737/stp-114202510

Received April 11, 2025
Accepted August 28, 2025

DETECTING GROUPS OF EIGENFREQUENCIES OF VERTICAL STANDING WAVES IN THE LAYERED STRUCTURE OF THE EARTH'S CRUST

A.R. Polyakov
Institute of Solar-Terrestrial Physics SB RAS, Irkutsk, Russia, polar@iszf.irk.ru

B. Tsegmed
Institute of Astronomy and Geophysics MAS, Ulaanbaatar, Mongolia, tseg@iag.ac.mn

Abstract. Using a novel signal processing technique — the method of correlation function of amplitude and phase fluctuations (APCF) — we have obtained the first spectra of equidistant frequency (EF) groups in records of background seismic oscillations. This method has previously been successfully applied to the analysis of resonant oscillations in Earth's magnetosphere-ionosphere system.

In the case of seismic oscillations, all peaks in the EF spectrum can be divided into two groups corresponding to eigenfrequencies of vertical standing waves of P and S types in the Earth's interior. The upper turning point of these waves lies at the free upper boundary of the Earth's crust, whereas the lower turning point is located at the boundaries between subsurface layers.

We demonstrate that this signal processing technique can serve as a new method for probing the layered structure of the Earth's subsurface. Specifically, it enables the determination of the depth and thickness of each layer, as well as the estimation of elastic properties (such as Poisson's ratio) of the geological material composing the layer. The findings have revealed that at the depth of ~2.7 km there are two layers of different solid substance 58 m and 140 m thick with Poisson's ratios of 0.231 and 0.187.

Keywords: signal processing technique, equidistant frequencies, eigenfrequencies, P- and S-type elastic waves.

INTRODUCTION

In the previous work [Polyakov, 2022], the method of correlation function of amplitude and phase fluctuations (APCF) has first been applied to mass processing of a large volume of terrestrial recordings of geomagnetic fluctuations in the frequency range from 0.1 to 3.0 Hz. The main purpose was to show to what extent the results are adequate, reliable, and match reality. In this paper, we try to expand the range of applicability of the APCF method, using it to process recordings of seismic vibrations in the Earth interior. Although issues of seismology are outside the scope of the journal Solar-Terrestrial Physics, the method of studying vibrations in layered media of different nature offers new possibilities for signal processing in various fields, including near-Earth plasma. Here we propose to focus on the problems related to methodology.

The APCF method [Polyakov, 2015, 2018] is based on the analysis of a specially constructed correlation function of amplitude and phase fluctuations and is designed to detect groups of equidistant frequencies in the broadband spectrum of the original signal.

At the first stage, the original signal in discrete form is converted into a small addition to the sinusoid of a given frequency. For such a signal at each time step i, we identify deviations of the amplitude $n_i(\Theta_i)$ and phase $\gamma_i(\Theta_i)$ from the amplitude and phase of the ideal sinusoid, where Θ_i is the sinusoid phase.

Next, cross- and autocorrelation functions of amplitude and phase fluctuations are found which are used to calculate the function

$$G(\tau) = \overline{\left[\gamma(\Theta)\gamma(\Theta-\tau)\right]}\,\overline{\left[n(\Theta)n(\Theta-\tau)\right]} - \overline{\left[\gamma(\Theta)n(\Theta-\tau)\right]}\,\overline{\left[n(\Theta)\gamma(\Theta-\tau)\right]}.$$

The overline means averaging over Θ; τ is the phase shift Θ.

The correlation function $G(\tau)$ has one interesting property. In the works listed above when processing simulated wave signals of various types in 1D and 2D resonators, it was convincingly shown that if there is a group of equidistant frequencies (EF) in the spectrum of the original signal, peaks appear in the structure of the function G, which periodically follow each other along the τ axis. From the position of the first peak, we can indirectly measure [Polyakov, 2018] the difference between two adjacent frequencies Δf of this equidistant group.

At the last stage of processing, all sequences of periodic peaks of the function $G(\tau)$ are identified and the difference Δf is measured for each of them. The final product of the processing of the original signal is a histogram of these differences.

For the traditional Fourier spectrum it is commonly supposed that the presence of a statistically significant peak in its structure means that the signal contains quasi-monochromatic oscillations at the frequency of this peak. In the APCF histogram, each peak corresponds not to one, but to a whole EF group in the spectral composition of the signal. The position of the peak on the Δf axis determines the difference between two adjacent frequencies of each such group. At the same time, the

APCF method cannot identify individual frequencies of the group. It is even impossible to establish in which part of the frequency range they are located and how many frequencies each group contains.

For natural broadband oscillations, eigenfrequencies of resonators should be considered as EF groups at those harmonic numbers when they become equidistant. Each standing 1D wave of the resonator forms one EF group in the traditional Fourier spectrum and corresponds to one peak in the Δf histogram. The final Δf histogram will sometimes be called the spectrum histogram of EF groups.

Polyakov [2022] has shown that if a natural signal is ground-based oscillations of the geomagnetic field, the source of such standing 1D waves is an Alfvén 2D resonator located at the outer edge of the plasmapause [Leonovich, Mazur, 1987].

The Earth interior has a layered structure in which P- and S-type elastic waves can be excited [Landau, Lifshitz, 1987; Bullen, 1966]. Obviously, standing 1D waves of both types can form inside each layer or several layers at a time. In this paper, we use the software program of the APCF method to process recordings of seismic vibrations. Analyzing the spectrum histogram of EF groups obtained for them for the first time, we try to figure out to which of the standing waves correspond certain peaks of this spectrum histogram.

1. RESULTS

For processing, we have used the recording of the December 13, 2016 earthquake from the seismic station Arshan (51°92' N; 102°42' E). The recording has three channels, i.e. three vibration components: N–S, E–W, and vertical. The data is presented in discrete form with a time step of 0.01 s. From the beginning of the recording to the beginning of the earthquake, there are background fluctuations with small deviations from the mean value in all the channels. The duration of this section is ~1 hr. Further, during the earthquake, these deviations increase dramatically by several orders of magnitude and last for 2–3 min until the end of the recording.

From the experience of applying the APCF method, it has been found [Polyakov, 2018, 2022] that the initial signal for processing should resemble a recording of a random process whose spectrum occupies a wide frequency range and is also similar to the noise spectrum. This is exactly how the oscillogram and the spectrum of background seismic fluctuations look like. In this situation, we must exclude the burst of deviations during the earthquake and accept only the recording of background fluctuations preceding it as the original signal.

This recording, however, proved to contain a very large monochromatic spectral component. Oscillograms, especially for the E–W and vertical components, look almost like ideal sinusoids with a frequency of 16.6 Hz. A peak is observed in the spectra at this frequency, which is more than two orders of magnitude higher than spectral peaks at all other frequencies.

For our APCF signal processing technique, one or two high-amplitude narrow peaks in the spectrum of the original signal produce very unpleasant noise. These peaks can severely distort or even create a false picture of the location of maxima in the spectrum histogram of EF groups obtained by our technique. In order for this seismic signal to be suitable for processing, it is necessary to somehow get rid of such peaks in the normal spectrum of the original signal.

In our case, the signal frequency range in processing by the APCF technique is set from 2 to 20 Hz. Removing noise at 16.6 Hz by conventional high-frequency filtering is barely acceptable as it will lead to a significant reduction in the frequency range, whereas for our technique the wider the range, the better.

We have therefore developed and applied a novel original method of equalizing all peaks of the spectrum of the original signal in height. A corresponding new procedure has been added to the signal preprocessing program.

At the beginning of the procedure, we define a complex Fourier transform function for the initial signal. In the plot of the modulus of this function versus frequency, we find frequencies and heights for each peak. As a result, we obtain a discrete envelope function of all spectrum peaks with an irregular frequency step. Let the frequency step be regular, equal to this step in the spectrum itself. Next, for each frequency step, we divide the real and imaginary parts of the Fourier function by the resulting envelope. At the end of the procedure, we perform the inverse Fourier transform for the modified complex function. The real part of the resulting complex time dependence is the transformed original signal in which almost all peaks in the spectrum are approximately equal in height.

After this procedure has been applied to our seismic signal, the abnormally high peaks in the spectrum mentioned above do not disappear completely, but simply become comparable in height to all other peaks. For such a signal, we can use the APCF processing technique without fear of noise in the final histograms. Moreover, it turned out that the spectral peak equalization procedure is useful even in the absence of very high peaks. When processing constructed signals similar to those used in [Polyakov, 2018], it was found that the use of this procedure often results in a decrease in the noise level in the spectrum histogram of EF groups.

We have divided the entire recording of seismic background fluctuations into nine 6-min intervals. It is obvious that fluctuations within each interval can be considered as a separate independent realization of the same wave propagation response process in the stable structure of the Earth interior. Unlike the magnetic field recording intervals [Polyakov, 2022], in this case we can average the spectra histograms of EF groups of each interval over the ensemble of all realizations in order to increase the statistical significance of the final result.

Each time interval contains discrete recordings of three components of the displacement of a point of the Earth's crust. For each component, the APCF technique produces one histogram of Δf differences, which, as mentioned above, can be considered a spectrum histogram of EF groups. Any such spectrum histogram is formed by peaks of eigenfrequencies of various standing P- and S-waves. According to [Landau, Lifshitz,

1987; Bullen, 1966], P- and S-waves contribute to each of the displacement components. There are no other standing waves in the Earth's subsurface. This means that the same peaks should take place in spectra histograms of different components. We do not examine these component spectra separately in detail, as was done in [Polyakov, 2022]. For each time interval, we determine only one spectrum histogram equal to the average of all components.

Figure 1, *a* presents such an averaged spectrum histogram of EF groups for the first time interval of recording of background seismic fluctuations. Along the vertical axis, n is the number of actual measurements of the difference between adjacent frequencies Δf in a particular EF group, n_0 is the total number of all attempts at these measurements. The ratio n/n_0 can serve as estimated probability of observation of a point on the curve for each Δf. For clarity and convenience of analyzing the location of peaks, the curve is smoothed by a running mean, and too slow variations are removed [Polyakov, 2022]. Therefore, in some sections the probabilities assume negative values. The differences Δf on the horizontal axis are given in dimensionless form, being multiplied by the time step of the original discrete signal $\Delta f \rightarrow \Delta f \Delta t$.

Figure 1, *a* displays a set of peaks. As noted above, each peak is determined by an EF group of a single standing 1D wave in the Earth interior. For most peaks significant in height, we drew vertical lines whose intersection with the horizontal axis gives the difference between two adjacent frequencies in the group for each peak. These differences [Hz] are listed in Table. Section 2 discusses the origin of all the marked peaks.

Also shown is a similar spectrum histogram of EF groups averaged over all time realizations (*b*) and a spectrum histogram of the N–S component averaged over the first three realizations (*c*).

If we trace from top to bottom along each vertical line, we can clearly see that for most peaks the position

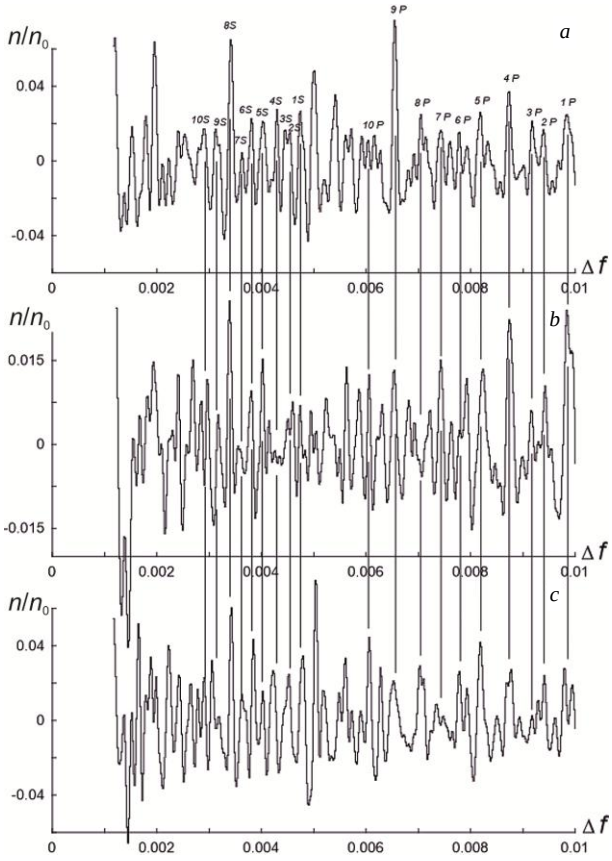

Figure 1. Spectra of EF groups — the final product of the APCF processing technique for recordings of background seismic vibrations from the Arshan station: the spectrum averaged over all components for the first time realization (*a*); the spectrum averaged over components and all time realizations (*b*); the N–S component spectrum averaged over the first three realizations (*c*). The values of Δf are given in the dimensionless form $\Delta f \rightarrow \Delta f \Delta t$, where Δt=0.01 s is the time step of the original signal

Characteristics of vertical standing waves in the Earth's subsurface experimentally measured from peaks of the spectrum histogram in Figure 1, *a*

i	$\Delta f_{i\mathrm{P}}$, Hz	$\Delta f_{i\mathrm{S}}$, Hz	h_i, km	Δh_i, m	$V_{i\mathrm{P}}/V_{i\mathrm{S}}$	λ_i/μ_i	ν_i
1	0.985	0.474	2.590	130	1.912	1.656	0.318
2	0.938	0.453	2.720	58	1.690	0.856	0.231
3	0.918	0.444	2.778	140	1.611	0.595	0.187
4	0.874	0.429	2.918	196	2.065	2.264	0.347
5	0.819	0.404	3.114	164	2.199	2.836	0.370
6	0.778	0.381	3.278	154	2.233	2.986	0.375
7	0.743	0.364	3.432	185	2.364	3.589	0.391
8	0.705	0.343	3.617	282	2.463	4.066	0.401
9	0.654	0.316	3.900	274	2.404	3.779	0.395
10	0.611	0.294	4.173				

of Δf on the horizontal axis (*b*, *c*) almost perfectly coincides with its position in panel *a*. Only two (number 8P and 4S) of the twenty marked peaks reveal significant deviations (panels *a*, *b*). It is also noticeable that the relative change in the height of the peaks during the transition from one number to another (*a*) is approximately the same as in panel *b*.

The correspondence between characteristics of most peaks (*a*, *b*) allows us to draw an important conclusion. The structure of the peaks in the spectrum histogram of EF groups for the first time realization of a seismic signal is, on average, exactly the same as for all other time realizations. We can consider the spectrum histogram (panel *a*) as a statistically reliable result.

The coincidence of the peak positions (*a*, *b*) indicates that even after averaging spectra histograms of one of the components over three time realizations we get almost the same initial standard spectrum histogram. This confirms the stability of all APCF signal processing procedures with respect to the final product (*a*).

Note that in panel *a* not all peaks are indicated by vertical lines. For example, the peak to the right of 5P, as well as the peak between 5P and 6P and the peak between 6P and 7P, cannot be considered reliable because they are absent or low in panel *b*. For now, we will not examine the remaining unmarked peaks between 10P and 1S, as well as to the left of 10S.

Let us pay attention to another important feature of the APCF method. At the very beginning of the work on this project, it became obvious that we cannot measure differences between adjacent frequencies Δf in the range of values from zero to infinity since this was technically impossible. We had to restrict ourselves to the finite range of these differences from 0.001 to 0.01 in dimensionless units. In addition to the peaks present (panel *a*), there may also be peaks with $\Delta f<0.001$ or $\Delta f>0.01$ that contribute to the spectrum of the original signal. Yet, they do not appear in the final spectrum histogram.

2. INTERPRETATION OF PROCESSING RESULTS

Assume that the Earth's subsurface in the region of the seismic signal monitoring station has a layered structure [Bullen, 1966]. Horizontally arranged layers can vary in thickness and composition of geological material. Boundaries between the layers can partially reflect and transmit elastic waves incident on them. A large number of different vertical standing waves should be observed in such a layered medium.

Any pair of boundaries between the layers blocks standing P- and S-waves since waves of both types are reflected at each boundary [Bullen, 1966]. Each standing wave features its own set of eigenfrequencies or an EF group in the Fourier spectrum of the seismic signal, which leads to the appearance of a separate peak (panel *a*).

Let us take a look at standing waves between two nearest boundaries. If the geological material is distributed evenly throughout the entire volume in this layer, the difference between adjacent eigenfrequencies for P- and S-type waves should be found from the formulas for first harmonic frequencies

$$\Delta f_{\mathrm{P}} = \frac{V_{\mathrm{P}}}{2\Delta h} = \frac{1}{T_{\mathrm{P}}}, \Delta f_{\mathrm{S}} = \frac{V_{\mathrm{S}}}{2\Delta h} = \frac{1}{T_{\mathrm{S}}},$$
$$V_{\mathrm{P}} = \sqrt{\frac{\lambda + 2\mu}{\rho}}, V_{\mathrm{S}} = \sqrt{\frac{\mu}{\rho}}, \quad (1)$$

where V_{P}, V_{S} are the velocities of P- and S-waves; ρ is the rock density; λ, μ are Lamé's elastic constants (compression modulus and shear modulus); Δh is the layer thickness; T_{P}, T_{S} are the periods of the first harmonic or the travel time between the upper and lower boundaries of the layer.

If the region of localization of a standing wave contains not one, but several layers at once, the total travel time is determined by the sum of travel times of the wave in each layer.

In our case, the seismic vibration sensor is located slightly below the free surface. This means that if a standing wave is located at a great depth, due to attenuation its contribution to the frequency spectrum of the vibrations recorded by the sensor will be negligible. The main contribution to this spectrum should be made by eigenfrequencies of those standing waves in which the upper turning point is on the free surface of the Earth's crust because this surface can fully reflect elastic waves and, above all, the seismic sensor is always located inside the region of localization of such standing waves. The lower turning point of these standing waves may be on one of the boundaries between rock layers.

For clarity, Figure 2, *a* offers a scheme of such standing waves. The vertical axis is downward and indicates the depth *h* of the Earth's subsurface. The horizontal axis represents the free surface of the Earth's crust, the boundary between the Earth's crust and the atmosphere $h_0=0$ deep. Horizontal lines in this scheme mark boundaries between the layers. Each such boundary and the layer located under it are assigned the number *i*. We have identified nine layers. The depth of the upper boundary of the layer with number *i* is denoted by h_i.

Vertical arrows indicate several regions of localization of standing waves between the upper and lower turning points. The lower turning point is located on the upper boundary of the layer with number *i*. We assign the same number to the corresponding localization region. In each region marked with an arrow, two P- and S-type standing waves should be observed. Differences between adjacent eigenfrequencies of such standing waves are designated respectively as $\Delta f_{i\mathrm{P}}$ and $\Delta f_{i\mathrm{S}}$.

From general considerations, we assume that for standing waves with multiple layers between turning points, as in the case of single layer (1), the eigenfrequency differences $\Delta f_{i\mathrm{P}}$ and $\Delta f_{i\mathrm{S}}$ coincide with the first harmonic frequencies. The period of this first harmonic is determined by the total travel time between the turning points through all layers. For it, in view of (1), we obtain the qualitative relation

$$T_{i\mathrm{P}} = \frac{1}{\Delta f_{i\mathrm{P}}} = \sum_{n=0}^{n=i-1} \frac{2\Delta h_n}{V_{n\mathrm{P}}},$$
$$T_{i\mathrm{S}} = \frac{1}{\Delta f_{i\mathrm{S}}} = \sum_{n=0}^{n=i-1} \frac{2\Delta h_n}{V_{n\mathrm{S}}}, \quad (2)$$

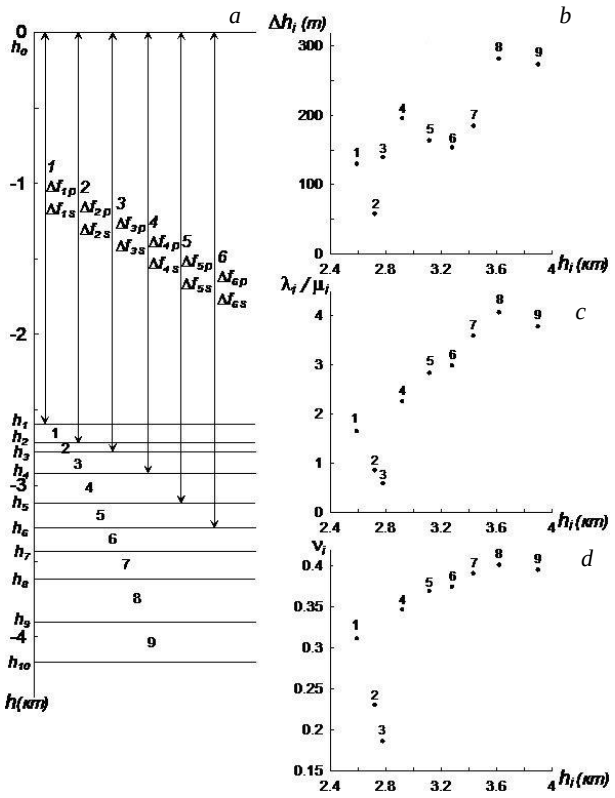

Figure 2. Scheme of vertical standing P- and S-waves and the alternation structure of horizontal layers of geological material in the Earth's crust, which we employed to interpret the locations of peaks in the spectra of EF groups (*a*); dependences of thickness, the ratio between Lamé's elastic constants, and the Poisson ratio of each layer on the depth of its upper boundary (*b*–*d*)

where n stands for the numbers of all layers located above the layer with number i; Δh_n, $V_{n\mathrm{P}}$, $V_{n\mathrm{S}}$ are the thickness and wave velocities of these layers.

For a pair of standing P- and S-waves with number i, the distance between the turning points is the same; this means, according to (2), that the ratio of $\Delta f_{i\mathrm{P}}$ to $\Delta f_{i\mathrm{S}}$ should be equal to the ratio between layer-average velocities of these waves within the region. As observed in [Bullen, 1966], this ratio between velocities in the Earth's subsurface, if rounded to an integer value, can be considered equal to ~2, i.e. $\Delta f_{i\ \mathrm{P}}/\Delta f_{i\mathrm{S}} \approx 2$.

Eigenfrequencies of standing waves (Figure 2, *a*) are almost ideally suited for interpreting positions of peaks on the horizontal axis of the spectrum histogram of EF groups obtained for background seismic vibrations.

Indeed, it is clearly seen in Figure 1, *a* that all the peaks indicated by vertical lines are divided into two separate groups. For the first group, located on the right, the frequency difference interval is 0.006–0.01; for the second, 0.0028–0.047; i.e., for the second group, the interval boundaries are about two times smaller than for the first. This strongly supports the fact that the first and second groups are caused by standing waves of P- and S-types respectively (see Figure 2, *a*). In Figure 1, *a*, the peaks of the first group are denoted by the *i*P indices; and the peaks of the second group, by *I*S.

In addition, it is also necessary to note the local property of the peaks. Figure 1, *a* clearly shows that in the P group, peaks 2P and 3P are located close to each other in the overall maximum. Obviously, their location indicates that these peaks are determined by eigenfrequencies of standing P-waves reflected upward from the upper and lower boundaries of a very thin layer (number 2) (see Figure 2, *a*).

In the series of S peaks, we can see a very similar maximum consisting of two peaks 2S and 3S, whose position on the horizontal axis in Figure 1, *a* is two times smaller than the position of peaks 2P, 3P. The gap between 2S and 3S is also ~2 times smaller than the gap between 2P and 3P. The gap is so small that peaks 2S and 3S almost merge with each other. This fact strongly supports that these peaks are caused by S-type standing waves. The waves are reflected respectively from the upper and lower boundaries of the aforesaid thin rock layer number 2.

Thus, the relative position of peak pairs 2P, 3P and 2S, 3S and the gap between the peaks of each pair clearly shows that for layer 2 each boundary gives two standing waves, P and S type. This conclusion indirectly confirms the applicability of the standing wave scheme (see Figure 2, *a*) for interpreting all peaks indicated by vertical lines in Figure 1, *a*.

In Figure 1, *a*, pairs of standing P- and S-waves reflected from the upper and lower boundaries of layer 2 correspond to peaks 2P, 2S and 3P, 3S. In Figure 2, *a*, each such pair of standing waves is denoted, as already mentioned above, by one vertical arrow to the upper and lower boundaries of layer 2.

By analogy, we simply have to assume that the other peaks marked with vertical lines in Figure 1, *a* are also formed by pairs of standing P- and S-waves reflected from the boundaries of other layers. To the right of 2P and 2S: peaks 1P and 1S should correspond to a pair of standing waves reflected from the upper boundary of layer 1. To the left of 3P and 3S: peaks 4P and 4S come from waves reflected from the upper boundary of layer 4; and peaks 5P and 5S, from layer 5. All these standing waves are exhibited in Figure 2, *a*. The last peak pair 10P and 10S corresponds to the reflection of waves from the upper boundary of layer 10.

Table presents exact differences (in hertz) $\Delta f_{i\mathrm{P}}$, $\Delta f_{i\mathrm{S}}$ of peak pairs for all the layer numbers considered, measured from their position on the horizontal axis Δf in Figure 1, *a*. In the velocity ratio column, we see that for all i numbers $V_{i\mathrm{P}}/V_{i\mathrm{S}} \approx 2$. This also indirectly confirms that the peaks marked in the spectrum histogram correspond to the eigenfrequencies of the standing P- and S-waves in Figure 2, *a*.

In Figure 1, *a*, the last peak pair with number i=10 is peculiar to the waves reflected from the upper boundary of layer 10, yet the lower boundary of this layer is missing and we do not see it in Figure 2, *a*. In this case, when analyzing the spectrum histogram of EF groups in Figure 1, *a*, we found nine separate layers that are most likely composed of different material.

Peaks 1P and 1S in Figure 1, *a* belong to standing waves with a lower turning point at a depth h_1 at the upper boundary of the first layer. In Figure 2, *a*, we do not see any other layers above it. However, this does not mean that they do not exist, it is just the Δf peaks in

Figure 1, *a*, which correspond to standing waves reflecting from higher layers, do not fall within the prescribed range of these differences. Therefore, such peaks, as mentioned earlier, are not present in Figure 1.

If in (2) the velocity of P-waves in different layers is replaced by the velocity averaged over each layer V_{aver}, we can obtain a relation for approximately determining the depth of the upper boundary of each layer.

$$h_i = \sum_{n=0}^{n=i-1} \Delta h_n = \frac{V_{\text{cp}}}{2\Delta f_{i\text{P}}}. \quad (3)$$

Volvovsky [1973] provides extensive tables of the results of measurements of wave velocities in different geographical regions. The measurements were carried out by the well-known method of deep seismic sounding with industrial explosions. From these tables for the Siberian platform of the Irkutsk Amphitheater in the sedimentary layer of the Earth's crust, we find V_{aver}=5.1 km/s. In a more recent paper [Dzhurik et al., 2024], at the same depth we have a similar average velocity V_{aver}=5.0 km/s. Substituting this velocity, as well as the values of $\Delta f_{i\text{P}}$ from Table in (3), we obtain the depth of the upper boundary of each layer. The difference $\Delta h_i = h_{i+1} - h_i$ is the thickness of the layer with number i. The results of the calculations of h_i and Δh_i are included in Table.

Figure 2, *b* illustrates the dependence of Δh_i on h_i. Numbers for each point indicate the layer number. The first and last layers have a depth of 2.6 and 4 km respectively, and the thickness of the layers varies over a fairly wide range Δh_i=60÷280 m.

Note that the velocity value that we took from [Volvovsky, 1973; Dzhurik et al., 2024] may differ from the real average layered velocity near the Arshan seismic station. It is, nonetheless, obvious that this difference should not be too large, and the calculated layer depth and thickness approximately match the real values.

For two adjacent peaks in Figure 1, *a* in the P- and S-groups, in view of (2), we have:

$$T_{(i+1)\text{P}} - T_{i\text{P}} = \frac{2\Delta h_i}{V_{i\text{P}}}, \; T_{(i+1)\text{S}} - T_{i\text{S}} = \frac{2\Delta h_i}{V_{i\text{S}}}.$$

This enables us to determine a number of important characteristics of the material that makes up the layers we have identified. For each layer with number i

$$\frac{V_{i\text{P}}}{V_{i\text{S}}} = \frac{\Delta f_{(i+1)\text{P}} \Delta f_{i\text{P}} \left(\Delta f_{(i+1)\text{S}} - \Delta f_{i\text{S}}\right)}{\Delta f_{(i+1)\text{S}} \Delta f_{i\text{S}} \left(\Delta f_{(i+1)\text{P}} - \Delta f_{i\text{P}}\right)},$$
$$\frac{\lambda_i}{\mu_i} = \left(\frac{V_{i\text{P}}}{V_{i\text{S}}}\right)^2 - 2, \; \nu_i = \frac{\lambda_i}{2\left(\lambda_i + \mu_i\right)}, \quad (4)$$

where ν_i is the Poisson ratio of the layer material; λ_i/μ_i is the ratio between Lamé's elastic parameters in the layer.

Substituting $\Delta f_{i\text{P}}$, $\Delta f_{i\text{S}}$ from Table in (4) yields characteristics of the elastic properties of the material of each layer, which are also tabulated. it is significant that unlike the method of determining the layer depth and thickness (3) in (4), we do not use the characteristics of the medium measured by other seismological methods. It can be assumed that in this case the accuracy of the layers' elastic parameters depends only on how accurate our signal processing technique is.

Figure 2, *c*, *d* plots λ_i/μ_i and ν_i as function of depth of the upper boundary of the layer h_i.

There is a curious result, especially noticeable in panel *d*. Almost all points form a smooth line, only points 2, 3 deviate significantly from it. The average Poisson ratio for points 4–9 is 0.35. It follows from online tables that substances such as aluminum, brass, and copper have approximately the same values, i.e. they are not very hard and brittle, but also not very soft and plastic such as lead and tin (ν=0.44).

Layer 2 has a Poisson ratio ν_2=0.23. This value corresponds to much harder and more brittle substances such as steel (ν=0.25), cast iron (ν=0.22), concrete (ν=0.20). Layer 2 is located at a depth h_2=2.72 km and has a thickness h_2=58 m. For layer 3, we obtain ν_3=0.19, h_3=2.78 km, and Δh_3=140 m from Table. The Poisson ratio in this layer is even lower and is peculiar, for example, to quartz glass ν=0.17 or basalt ν=0.12.

Note that the coefficients ν_i we have obtained do not allow us to unambiguously indicate the substance that makes up each layer, since different rocks can have the same value of ν_i. However, in this case, it is highly likely that layers 2 and 3 are granite and basalt plates respectively, which, according to [Bullen, 1966], should be located below the sedimentary layer. In this case, near the Arshan station these plates or layers are located at a depth of ~3 km.

Figure 2, *d* also indicates that the Poisson ratio increases smoothly with increasing depth in layers 4–9. This might be related to the temperature gradient. Referring to Figure 2, *d*, the temperature effect appears to be noticeably below the basalt layer at 3–4 km depths.

Note that this work is the first attempt to apply the novel technique to processing of recordings of background seismic vibrations. In the future, we should try to confirm the results obtained by processing other similar recordings from different seismic stations, if possible. If we can clearly demonstrate that each time the peaks in spectra of EF groups are determined by groups of eigenfrequencies of vertical standing waves, similar to those shown in Figure 2, *a*, we will get a useful, proven, and not very expensive sounding method. Detecting layers of different geological material, finding the depth and thickness of these layers provides valuable information on the structure of the Earth's subsurface. Moreover, we will be able to determine the Poisson ratio, which characterizes the elastic properties of the geological material of each layer.

CONCLUSION

1. For the first time, a 1 hour recording of background seismic fluctuations has been processed by the novel original APCF technique. It can identify groups of equidistant frequencies, which are present in the spectrum of the original signal, and can measure the difference between two adjacent frequencies Δf in a group. The final product of the processing is a spectrum histogram of Δf set.

In the traditional spectrum, the presence of a peak at a certain frequency means that fluctuations of this frequency occur in the original signal. In our spectrum histogram, each peak corresponds not to one, but to a whole group of equidistant frequencies in the original signal. The location of the peak on the horizontal axis gives us not a separate frequency but the difference of two adjacent frequencies characteristic of the whole group.

In our case, by the EF group in the spectrum should be meant eigenfrequencies of any one of the standing waves excited in the layered structure of the Earth's subsurface.

2. Analysis of the obtained spectrum histogram (see Figure 1) quite convincingly shows that most of the observed peaks are caused by eigenfrequencies of P- and S-type vertical standing waves. The scheme of these waves is given in Figure 2, *a*. The main thing about it is that each pair of standing P- and S-waves has the same turning surfaces. The upper surface is always located at the boundary of the Earth's crust and the atmosphere, and the lower surface coincides with one of the boundaries between layers of different geological material.

3. It has been found that if we accept this interpretation of the spectrum-histogram peaks, we can determine the approximate depth of the boundaries between the layers and the Poisson ratio of substance in each layer, i.e., we can obtain a new method for experimental detection of the layered structure in the Earth interior.

However, at this stage it is obvious that the development of a new method can be discussed only if the features of the location of peaks in spectra histograms identified in this work are repeatedly confirmed in processing other records of seismic background fluctuations by the APCF method at different stations at different times.

We would like to express our gratitude to BF FRC GS RAS for providing recordings of background seismic fluctuations from the Arshan station.

The work was financially supported by the Ministry of Science and Higher Education of the Russian Federation.

REFERENCES

Bullen K.E. *An Introduction to Theory of Seismology*. Moscow, MIR Publ., 1966, 460 p. (In Russian).

Dzhurik V.I., Bryzhak E.V., Serebrennikov S.P., Kakourova A.A. Identification of the features of the influence of heterogeneous-velocity ground layers on large-earthquake effects in the Mongolian-Siberian region. *Geodynamics and Tectonophysics*. 2024, vol. 15, no. 6. DOI: 10.5800/GT-2024-15-6-0793. (In Russian).

Landau L.D., Lifshitz E.M. *Theory of Elasticity. Theoretical Physics*. Moscow, Nauka Publ., 1987, vol. 7, 246 p.

Leonovich A.S., Mazur V.A. Dynamics of small-scale Alfvén waves in magnetospheric resonator. *Fizika plazmy* [Plasma Phys.]. 1987, vol. 13, iss. 7, pp. 800–810. (In Russian).

Polyakov A.R. Relationship of peaks of correlation functions of amplitude and phase fluctuations with eigenfrequencies in oscillation spectrum. *Sol.-Terr. Phys.* 2015, vol. 1, iss. 3, pp. 62–71. DOI: 10.12737/10455.

Polyakov A.R. Detecting groups of equidistant frequencies in spectra of geomagnetic pulsations. *Sol.-Terr. Phys.* 2018, vol. 4, iss. 4. pp. 33–41. DOI: 10.12737/stp-44201805.

Polyakov A.R. Structure of groups of eigenfrequencies in spectra of geomagnetic pulsations in the nightside magnetosphere. *Sol.-Terr. Phys.* 2022. vol. 8, iss. 3, pp. 46–50. DOI: 10.12737/stp-83202207.

Volvovsky I.S. *Seismic Studies of the Earth's Crust in the USSR*. Moscow: Nedra, 1973, 208 p.

Original Russian version: Polyakov A.R., Tsegmed B., published in Solnechno-zemnaya fizika. 2025, vol. 11, no. 4, pp. 106–113. DOI: 10.12737/szf-114202510.

How to cite this article

Polyakov A.R., Tsegmed B. Detecting groups of eigenfrequencies of vertical standing waves in the layered structure of the Earth's crust. *Sol.-Terr. Phys.* 2025, vol. 11, iss. 4, pp. 97–103. DOI: 10.12737/stp-114202510.